



## Application of Nanocomposites of Chitosan and Neptune Grass- Biosynthesized Selenium Nanoparticles as Edible Coatings for Preserving Citrus Fruits

Aya M. Ebaid<sup>1</sup>, Hoda Mahrous<sup>1</sup> and Mohamed F. Salem<sup>2</sup>

<sup>1</sup>Department of Industrial Biotechnology, Faculty of Biotechnology, University of Sadat City, El Sadat City 22857, Egypt.

<sup>2</sup>Department of Environmental Biotechnology, Faculty of Biotechnology, University of Sadat City, El-Sadat City 22857, Egypt.

Received: 05 Feb. 2026

Accepted: 20 Mar. 2026

Published: 30 Mar. 2026

### ABSTRACT

Nanobiotechnological techniques can be used to effectively solve the problems associated with contamination and spoilage of food products. Rapid and environment-friendly approaches for synthesis of nanocomposites consisting of chitosan nanoparticles (Cht), neptune grass extract 'Posidonia oceanica' (NG) and selenium nanoparticles generated by NG (SeNPs) were envisaged, and their use as potential antifungal and edible coatings (ECs) and biopreservatives of citrus (orange) fruits was investigated. SeNPs were biosynthesized using NG, and the conjugation between SeNPs and Cht nanocomposites was carried out. Characterization techniques such as FTIR screening, structure and optical analysis of biosynthesized nanomaterials were used. Antifungal activity of biosynthesized nanomaterials against *Penicillium digitatum* fungal isolates was determined. The potential antifungal activities of nanomaterials were utilized in making ECs for the preservation of oranges (*Citrus × tangelo*). Biosynthesis of SeNPs using NG was highly successful, with an average diameter of 13.82 nm; NG/SeNPs showed homogenous spherical structures with even distribution. Average diameter of biosynthesized Cht/NG/SeNPs was found to be 171.55 nm. The role of biochemical compounds in the synthesis and reaction of nanomaterials is evident from their infrared analysis. The antifungal activities of nanomaterials were seen against all of the tested strains of fungi. In particular, for the cases of *P. digitatum* isolates, all agents and nanocomposites possessed good fungicidal capacities; however, the highest was observed in Cht/NG/SeNPs nanocomposites, which performed way better than the fungicidal efficacy of traditional fungicides. Symptoms of green mold were eradicated completely after applying Cht/NG/SeNPs nanocomposite-based ECs on an infected orange fruit. This study can contribute toward future utilization of biosynthesized compounds for producing edible coatings and antifungal nanocomposites on citrus fruits.

**Keywords:** Antimicrobial, green synthesis, bioactivity, meat preservation, neptune grass.

### 1. Introduction

Citrus has a number of valuable fruit types, which can easily be affected by various microbial infections because of their rich nutrients and high water content (Wang *et al.*, 2020). In general, the acidity of citrus nature varies within pH 2.2–4.0, and fungi have been observed to be the main cause of their infection and deterioration (Cheng *et al.*, 2020); fungi may affect them at any stage of their life. One example of such disease-causing organisms is *Penicillium digitatum*, a necrotrophic fungus known to cause the main postharvest spoilage in citrus fruits under the name of green mold. Such damage has great economical impacts as the losses reach  $\geq 90\%$  of the entire postharvest damages (Cheng *et al.*, 2020; Tayel *et al.*, 2009). For instance, despite being among one of the top citrus producers, the tropical climate of Egypt makes the exported quantities of their fruits very low because of fungi contamination (FAOSTAT, 2020).

**Corresponding Author:** Aya M. Ebaid, Department of Industrial Biotechnology, Faculty of Biotechnology, University of Sadat City, El Sadat City 22857, Egypt.

As a result of restriction regulation, carcinogenic potential and high toxicity, long-lasting decomposition period, ecological impact, development of resistant strains of fungi, and increased consumer concern over chemical residue in vegetables, the application of synthetic or chemical fungicides received more attention (Wang *et al.*, 2020; Tripathi and Dubey, 2004). As such, the utilization of natural products and biological strategies (such as antagonistic microorganisms, bioactive natural compounds, and nanobiomaterials) was considered highly attractive in terms of being eco-friendly and effective in combating postharvest diseases caused by fungi (Tripathi and Dubey, 2004; Tayel *et al.*, 2016; Kharchoufi *et al.*, 2018).

Nanotechnology and nanoparticles (NPs) are currently being utilized in almost all human-oriented fields; these include biomedicine, chemistry, nutrition, biology, optics, mechanics, agriculture and environmental fields (Sharma *et al.*, 2018; Kumar *et al.*, 2021). The NPs are highly utilized in the manufacture, process and storage of human foodstuffs, starting from agriculture to the production and display of food items to consumers (Khot *et al.*, 2012; He *et al.*, 2019). Due to the unique properties of NPs, such as increased surface area, extremely small sizes, enhanced penetrative power and shapes, these nanomaterials show special qualities when compared to bulk particles. The usual NPs synthesis method which involves the physical and chemical method poses many risks since the physical method involves energy consumption and expensive processes while the chemical approach is ecologically unsafe (Saratale *et al.*, 2018). On the other hand, the utilization of biomaterials such as bacteria, algae, polymers, plant extracts and its derivatives to facilitate biosynthesis of NPs may be an effective solution to these problems (Ganachari *et al.*, 2019; Bahrulolum *et al.*, 2021). Selenium is one of those elements which plays different roles biologically in addition to being a cofactor of antioxidant enzymes protecting the human body against free radicals (Yu *et al.*, 2023). There are many pharmacological uses of selenium including its role in immunomodulation, cellular metabolism, and regulation of thyroid hormone metabolism (Rao *et al.*, 2022). It also has properties like being antibacterial, antifungal, antiviral, anticancer, and antioxidative in nature. Selenium has been tested in terms of effectiveness against kidney, liver, and heart damages caused due to oxidation (Khurana *et al.*, 2019). Selenium nanoparticles (SeNPs) compared to inorganic selenium have many advantages, including low toxicity, high chemical stability and good biocompatibility (Zhai *et al.*, 2017). Moreover, since smaller particles have a lower metabolic activity and are more effectively agglomerated in biological tissues, selenium nanoparticles (SeNPs) also display size-dependent responses (Nayak *et al.*, 2021).

Active substances' absorptions and bioavailability can be increased by converting their formulations into the nanoscale (Zhang *et al.*, 2006). Antimicrobial efficiency of selenium nanoparticles was greater than that of inorganic selenium (Hariharan *et al.*, 2012). There are certain advantages of using SeNPs over conventional antimicrobial agents against resistant mechanisms adopted by bacteria such as slow drug penetration, rapid efflux, and biofilm development (Pelgrift and Friedman, 2013).

Bioactivities and bioavailabilities of SeNPs in an aqueous medium were low due to the tendency of these SeNPs to form large aggregates (Khurana *et al.*, 2019; Nayak *et al.*, 2021; Yu *et al.*, 2023). SeNPs and organic polymer nano-composite particles (NCs) were fabricated for increased bioactivities such as prolonged delivery and organ-specific targeting (Torres *et al.*, 2012; Chen *et al.*, 2015). Being non-toxic, biocompatible, easily available, renewable, and multifunctional, chitosan is considered one of the best choices among polymers to obtain the NCs having physiological effects (Tayel *et al.*, 2020). Chitosan nanoparticles have a unique feature that helps increase the permeability of hydrophilic substances (Ferreira Meneses *et al.*, 2023). Bioactivities of metallic nanoparticles, like antimicrobial, anticarcinogenic, anti-inflammatory, antiviral, and antioxidant activities, were found to be increased by Cht (Jha and Mayanovic, 2023).

Three leading approaches have been developed for the synthesis of SeNPs: chemical, biological and physical (Bahrulolum *et al.*, 2021). Since it is biocompatible, cost effective and eco-friendly, so the biological method stands out as a preferred technique for producing pharmaceutical materials (Nayak *et al.*, 2021; Yu *et al.*, 2023). Fungi, algae, bacteria and plants can generate SeNPs by biogenic or green synthesis together with metabolites in the form of stabilizers and reducing agents (Nayak *et al.*, 2021; Bahrulolum *et al.*, 2021).

As discussed earlier, environmental species such as *Posidonia oceanica*, commonly known as Neptune grass (Posidoniaceae) (Vacchi *et al.*, 2019), can also have a role in metallic nanoparticles

production (Ammar *et al.*, 2021). Ng extract of *P. oceanica* had phenolic acids, including 4-hydroxybenzoic acid, coumaric, gentisic, cinnamic and chicoric acids and ferulic acids; flavonoids (quercetin, kaempferol), myricetin (Haznedaroglu and Zeybek 2007). via their stabilizing/ reducing activity for biosynthesis of nanoparticles.

Due to its promising uses, *P. oceanica* has gained attention in health care products particularly because of the antiradical and antioxidant properties of its phenolic compounds.

The storage life of food products has greatly increased through the invention of Edible Coating (EC), a form of packaging technology. According to the definition, "Edible coatings refer to thin layers of substances covering food products and edible that become part of the foods themselves." Edible coatings from natural sources are able to increase the quality of food products in addition to being environmentally friendly. EC was used to preserve fresh fruits, meat products, vegetables, and other food products using proteins, lipids, polysaccharides, and many other biopolymers.

There is no reported scientific studies on the biosynthesis of the Cht/NG/SeNPs nanocomposites by using *P. oceanica*. Therefore, our aims include: i) Synthesis of Cht/NG/SeNPs; ii) Study the physiochemical and structural properties of Cht/NG/SeNPs nanocomposites; iii) Antifungal activity of biosynthesized nanocomposites against *P. digitatum* green mold; iv) Evaluation of biopreservative properties of nanocomposites as coating agents.

## 2. Materials and Methods

### 2.1. *Posidonia oceanica* collection and identification

The leaves of Neptune grass (*Posidonia oceanica*) were collected from flowering grass samples near Marsa Matrouh in the Mediterranean coast of Egypt (Figure 1). The identification and cleaning of the grass samples was done by "Faculty of Aquatic and Fisheries Sciences, Kafrelsheikh University." The grass samples were first washed thoroughly with distilled water (DW) to ensure the elimination of all sands and salts. The grass samples were dried for 54 hours at 43 °C and then crushed at RT.



**Fig. 1:** Neptune grass (*Posidonia oceanica*) bloom and close image of plant materials

### 2.2. Preparation of Neptune grass (NG) extract

*P. oceanica* leaf powder was extracted by macerating it in ten times 70% ethanol for a whole night at 37±1 °C while stirring (190 x g). Following filtration, the Neptune grass extract (NG) was vacuum-evaporated at 42±1 °C until it was completely dry. After being reconstituted in DW, the dry NG powder was vortexed and filtered (Abd-Elraoof *et al.*, 2023).

### 2.3. Phytosynthesis of SeNPs using Neptune grass extract

10 mM Na<sub>2</sub>SeO<sub>3</sub> solutions and an equal volume of NG (0.1%, w/v) were mixed and agitated at room temperature for 35 minutes at 720 x g in the dark. The preceding solutions were then gradually

supplemented with an aqueous solution of ascorbic acid (50 mM). The reaction mixtures were agitated for 60 minutes using a magnetic stirrer to complete the reduction process. The solution's color changed from pale yellow to orange-red, indicating that NG had synthesized SeNPs. The resulting nanoparticles (NPs) were lyophilized, recovered by centrifugation (10,700 x g for 18 min), and stored at room temperature (Barletta *et al.*, 2015). To remove the majority of capping NG, five consecutive DIW-centrifugation cycles were used to obtain the plain SeNPs.

#### 2.4. Extraction of chitosan

*Erugosquilla massavensis* (mantis shrimp) shell waste was used for the extraction of chitosan. Shell waste from "Seafoods processing plants, Kafrelsheikh University, Egypt" was collected and dried in DW for 20 hours at  $55 \pm 3$  °C. Chitosan extraction followed after pulverizing the shells. This involved demineralization using 16x1M HCl for 12 hours at room temperature, deproteinization using 16x1M NaOH for 12 hours at room temperature, and deacetylation using 18x55% NaOH solution for 95 minutes at 115 °C. The resulting powder was kept for further analysis after every stage where it had been completely washed and dried in DW (Benhabiles *et al.*, 2012; Tayel *et al.*, 2020).

#### 2.5. Synthesis of Cht/NG/SeNPs nanocomposites

To achieve concentrations of 1% (w/v), chitosan powder was dissolved in 0.15% (v/v) aqueous acetic acid. After preparing a 0.1% NG/SeNPs solution in DW, equal volumes of the aforementioned solutions were combined and agitated (480 x g, 45 min). Within an hour, a 0.5% concentration of sodium tri-polyphosphate (TPP) was added to 50 mL of the combination solution while stirring continuously (Huang *et al.*, 2004). The produced Cht from chitosan, NG, and SeNPs was harvested using three centrifugations (10700 x g, 28 min) with DW washing before being lyophilized. The TPP solution was added to the chitosan solution for the plain Cht production, and the following procedures were followed.

After lyophilizing all of the nanometals and NCs, their powders were reconstituted in DW at a 1.0% concentration (w/v), sonicated for 15 minutes, and used for additional analysis and tests following the necessary dilutions with DW.

#### 2.6. Characterization

##### 2.6.1 Fourier transform infrared spectroscopy (FTIR) analysis.

After being combined with 1% KBr, the powders of NG, SeNPs, Cht, and Cht /NG/SeNPs nanocomposite were exposed to FTIR screening in the 4000-450  $\text{cm}^{-1}$  area using a "Thermo Fisher, Nicolette IS10, Waltham, MA" device.

##### 2.6.2 UV analysis

The UV-visual spectroscopy examination "Shimadzu, UV-2450, Japan" within the 200–800 nm absorbance range was another method of characterizing NG-synthesized SeNPs.

##### 2.6.3 Particle's Sizes (Ps) and Zeta ( $\zeta$ ) Potential of Nanomaterials

The Ps and  $\zeta$  potentials of the nanoparticles (Cht, NG/SeNPs, and Cht /NG/SeNPs) were determined by DLS "Dynamic light scattering" technique by the help of Malvern 3000 HS Zetasizer (Malvern, UK). The Ps/ $\zeta$  potentials of the samples were studied at room temperature in the range from -200 mV to +200 mV upon sonication of the solutions in DW (0.02%) for 20 min at 23 Hz (ElSaied *et al.*, 2021).

##### 2.6.4 Electron microscopy screening

NCs (Cht/NG/SeNPs) with respect to the Ps, morphology, and dispersibility were studied by means of SEM ("Scanning electron microscopy, JEOL, JSM-IT100, Tokyo, Japan") and TEM ("Transmission electron microscopy, Leica-Leo 0430; Cambridge, UK"). After ultrasound treatment for 12 minutes, NC was deposited onto carbon-coated copper grids, dried in a vacuum for 28 minutes, and then subjected to TEM at 20 kV. Alternatively, Cht, NG, and SeNPs NC was lyophilized, coated with palladium and gold, mounted on SEM discs, and observed using SEM at 8-10 kV (Marrie and Costerton, 1984; Tayel *et al.*, 2010).

## 2.7 Green mold isolates

The particle size, morphology, and dispersity of NCs (Cht/NG/SeNPs) were measured by SEM ("Scanning electron microscopy, JEOL, JSM-IT100, Tokyo, Japan") and TEM ("Transmission electron microscopy, Leica-Leo 0430; Cambridge, UK"). The NC solution following 12 min ultrasonication was deposited onto C-coated copper grids and subjected to vacuum dehydration for 28 min and analyzed by TEM at 20 kV. On the other hand, NC of Cht, NG, and SeNPs were freeze-dried, coated with palladium and gold, mounted on SEM adhesive disks, and imaged by SEM at 8-10 kV.

## 2.8. In Vitro Evaluation of Antifungal Activity

The effect of Cht, NG, NG/SeNPs, and Cht/NG/SeNPs on the antifungal activity against *P. digitatum* was tested by using in vitro analysis. The reference antifungal compound selected was imazilil from Sigma-Aldrich (Taufkirchen).

### 2.8.1. Well Diffusion (WD) method

The Agar WD method is widely used to evaluate the antifungal potentiality, particularly from natural compounds (Tayel *et al.*, 2010). The PDA plates were first inoculated and distributed with 100  $\mu$ L of fungal SS. A cork-borer was used to create wells with a diameter of 6 mm, and 50  $\mu$ L of each chemical (1% concentration in DW or imazilil in DMSO) was pipetted into each well. The inhibition zones (ZOI) surrounding the wells were measured in millimeters after the plates were incubated for 72 hours at 27°C in the dark (Pulido *et al.*, 2000).

### 2.8.2. Minimum Fungicidal Concentration (MFC).

The MFCs of the drugs tested (i.e., ChT, NG, ChT+NG, and ChT+NG+SeNPs) or imazilil in their dilution broth were assessed against the *P. digitatum* isolates as shown (Tayel *et al.*, 2016; Haghighi and Yazdanpanah, 2020). The PDB was combined with increasing concentrations of chemicals (from 10 to 100 mg/mL), along with *P. digitatum* SS isolates. The cultures containing the medium were incubated for eight days under aerobic conditions and then inoculated into new PDA plates. After seven days of incubation, the MFC for each chemical against fungal isolates was estimated based on no cellular development on the plates.

## 2.9 Antifungal Edible coating

### 2.9.1. Edible coating (EC) preparation

Modification of the method for preparation of the ECs as described by Tayel *et al.* (2009) was adopted. To put it succinctly, bioactive chitosan derivatives (i.e., chitosan itself, NG/SeNPs and Chitosan/NG/SeNPs) were dissolved in the acidified DW (pH 5) at their individual MFCs and glycerol 5% v/v was added to all solutions as a plasticizer.

### 2.9.2. Fruits treatment

The organically cultivated Minneola tangelo orange (*Citrus*  $\times$  tangelo) samples were collected from the Agricultural Research Centre, Giza, Egypt, the fruit average diameter was 8.7 $\pm$ 0.3 cm, without any mechanical damage or infections on their surface. Prior to coating, fruits were irrigated with DW, sanitized through soaking them in the NaOCl (5%) solution for 2.5 min, again washed by DW and then left for drying up. Minneola oranges were infected mechanically with wounding one site at equator using sterile blade (4 mm width X 3 mm depth). Wounded fruits were immersed in 1200 mL of Pd O fungal suspensions (SS) for 8 min (for artificial infection production), drained for 15 min, followed by aseptic air drying for 90 min. Then fruits were immersed in Cht-containing ECs (~ 1L) for 5 min under stirring conditions and RT air-drying. The oranges which were coated with Cht-free EC served as a control sample. EC-coated oranges were maintained in a sterile room (90% relative humidity) for 14 days at controlled RT. The diameter of fungal lesions (LD) was measured regularly during the inoculation period (Tayel *et al.*, 2009).

## 2.10. Statistical analysis

The experiments were carried out in duplicate, and SPSS V-20 software was used to calculate and compare the means and SD (standard deviations). One-way ANOVA was used to calculate the significance of the differences at  $p < 0.05$ .

## 3. Results and Discussion

### 3.1. Characterization of nanomaterials

#### 3.1.1 Visual examination

When *P. oceanica* extract was added, the color of the  $\text{Na}_2\text{SeO}_3$  solution changed from pale yellow to orange-red, as shown visually (Figure 2-1). After two hours, there were no additional color changes, however the color intensity did grow with time.

The appearance of one characteristic absorption peak, such as at 279 nm, in the UV-vis spectrum of NG-mediated SeNPs (Fig. 2-2) is indicative of the homogeneity of phycosynthesized particle size and is closely linked to the characteristic SPR "Surface plasmon resonance" of biosynthesized SeNPs (Pelgrift and Friedman, 2013; Kharchoufi *et al.*, 2018; Cheng *et al.*, 2020; Kumar *et al.*, 2021).

Benhabiles *et al.* (2012) also verified that the production of SeNPs using *Spirulina platensis* extract changed color from colorless to pale red. The high cellulose content (40%) and comparatively high extractive content of *P. oceanica* balls led to the production of SeNPs and the bioreduction of  $\text{Na}_2\text{SeO}_3$  into red  $\text{Se}^0$  (Torres *et al.*, 2012; Hariharan *et al.*, 2012; Yu *et al.*, 2023).

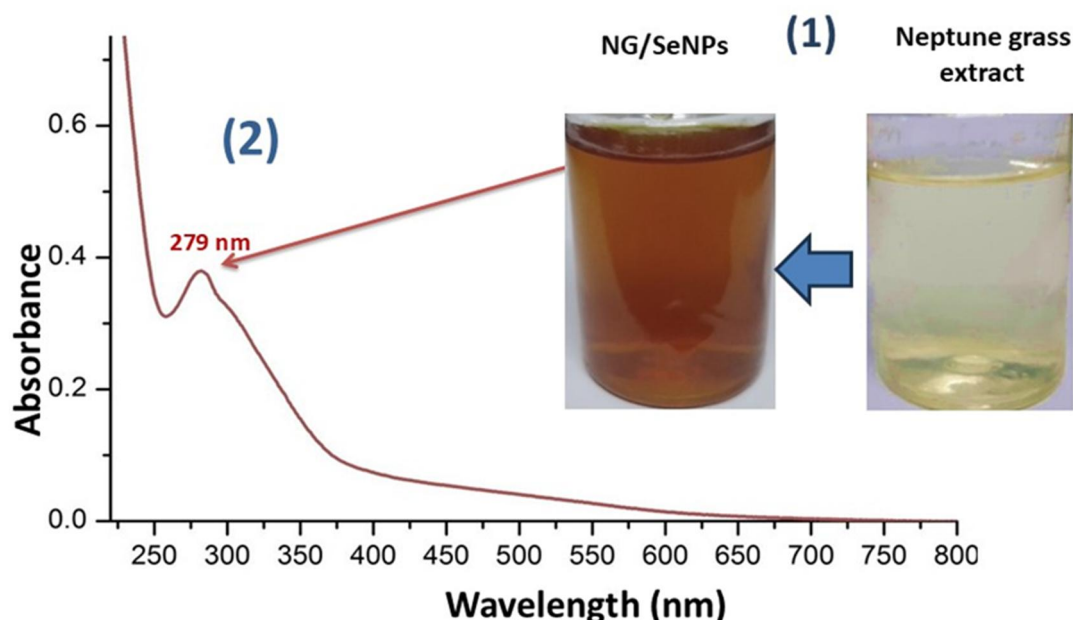


**Fig. 2:** The biosynthesis of SeNPs using Neptune grass extract as confirmed by changes in the solution's colour from pale yellow to orange red (1) and UV spectrum (2) after 2 h of treatment

#### 3.1.2. FTIR analysis

The wavelength for Cht in the infrared spectra shown in Fig. 3-Cht was observed to be at  $3426\text{ cm}^{-1}$ , indicating the presence of hydrogen bonding in O-H/N-H molecules. The typical bands for polysaccharides are those observed at wavelengths for the symmetric and asymmetric stretching vibrations of C-H at  $2921\text{ cm}^{-1}$  and  $2872\text{ cm}^{-1}$ , respectively [10, 11]. These are some of the biological bands identified for Cht:  $1153\text{ cm}^{-1}$  (asymmetric C–O–C bridge),  $1067\text{ cm}^{-1}$  and  $1024\text{ cm}^{-1}$  (C–O stretching),  $1654\text{ cm}^{-1}$  (stretching C = O of amide I),  $1321\text{ cm}^{-1}$  (stretching C–N vibrated),  $1412\text{ cm}^{-1}$  and  $1357\text{ cm}^{-1}$  ( $\text{CH}_2$  bending/ $\text{CH}_3$  symmetrical deformations). Bands at  $1153\text{ cm}^{-1}$  and  $1066\text{ cm}^{-1}$

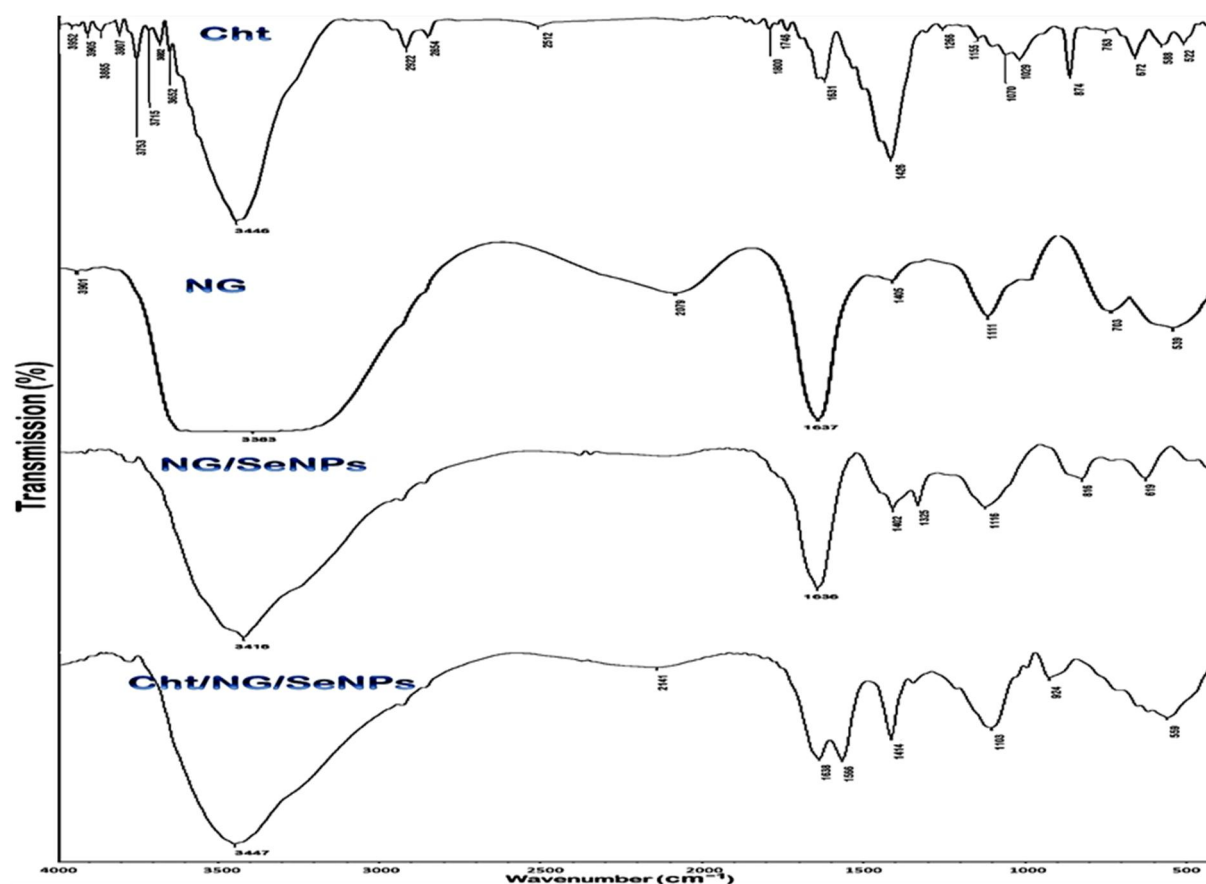


**Fig. 3:** Neptune grass extract (NG), nanochitosan (Cht), Neptune grass/SeNPs (NG/SeNPs), and Cht/NG/SeNPs nanocomposite were all analyzed using FTIR.

Fourier-transform infrared spectra (Figures 3–NG) for Neptune grass extract showed the presence of wide band in the region of 3600 to 3000  $\text{cm}^{-1}$  that suggested the existence of both -OH and -NH vibrations. Though the peak of 1423  $\text{cm}^{-1}$  was associated with -C-OH bend vibration that assisted in the symmetrical stretching of O-C-O vibration of carboxylate functional group important for the sorption process of metals, the peak observed at 1607  $\text{cm}^{-1}$  was attributed to amide -NH vibration. Vibration for ester group was identified in the frequency of 1273  $\text{cm}^{-1}$ . The intense vibration at 1046  $\text{cm}^{-1}$  shows the presence of alcohol group. As *Posidonia* is made up of lignin, cellulose, and hemicelluloses, some vibrations can be justified by their respective functional groups (Fortunati *et al.*, 2015; Boubakri *et al.*, 2017; Varma and Vasudevan, 2020).

The analysis of the NG/SeNPs spectrum was done in order to find the main players responsible for biosynthesis of the SeNPs in NG group (see Fig. 3 NG/SeNPs). It is obvious that the NG/SeNPs spectrum has an offsetting peak at 3426  $\text{cm}^{-1}$  towards 3482  $\text{cm}^{-1}$ , which confirms the establishment of Se binding with the groups of N-H and O-H, although the peak associated with C-H group in the NG spectrum at 2887  $\text{cm}^{-1}$  was completely ignored by NG/SeNPs. In addition to the above-mentioned properties of NG for SeNPs synthesis and reduction, it can be observed that the NG spectra revealed a significant change in the band at 1722  $\text{cm}^{-1}$  (N-H of amides and carbocyclic group) and the band at 1601  $\text{cm}^{-1}$  (aromatic rings C=C). In the NG/SeNPs spectra, the 1378  $\text{cm}^{-1}$  band corresponded to the 1439  $\text{cm}^{-1}$  band (aromatic rings in the NG spectrum). The formation of new vibrations due to the interaction between Se atoms and NG molecules can be seen through the formation of a number of intense peaks in the NG/SeNPs spectrum at 1603  $\text{cm}^{-1}$  and between 756–812  $\text{cm}^{-1}$  (Kannan *et al.*, 2014; Mellinas *et al.*, 2019).

The FTIR technique was applied to determine the functional groups participating in the SeNPs and Cht interaction based on the IR spectrum of Cht/NG/SeNPs nanocomposites (see Fig. 3: Cht/NG/SeNPs). The broad absorption band around 3226  $\text{cm}^{-1}$  corresponds to O-H stretching vibrations of carboxylic acids. The very narrow band centered at 2878  $\text{cm}^{-1}$  results from vibrations of

the C-H bond in alkanes. The narrow absorption band observed at 1297 cm<sup>-1</sup> is assigned to aromatic amines (C-N stretching) and nitro compounds (symmetric N-O stretching), while the minor band observed at 1023 cm<sup>-1</sup> refers to vibrations of aliphatic amines stretched stretch (Britto *et al.*, 2021).

FTIR spectroscopy confirmed that the bio-organics found in the extract of *P. oceanica*, including amino acids, esters, and the carbonyl/amide phytoconstituents of unsaturated ketones, could act as good capping or reducing agents for SeNPs (Liu *et al.*, 2013).

### 3.1.3. Particle Size and Zeta Potential ( $\zeta$ ) Analysis

Size and zeta potential are two important physicochemical properties of nanoparticles (Khan *et al.*, 2019). Particle sizes (Ps) of NG/SeNPs, Cht, and Cht/NG/SeNPs in Table 1 are 13.82, 162.16, and 171.55 nm, respectively. Based on the study by Khoerunnisa *et al.* (2021), the particle sizes of SeNPs were observed to be within the range of 3 to 18 nm. On the other hand, according to Ashraf *et al.* (2018), chitosan nanoparticles had a mean diameter of 109.59  $\pm$  10.11 nm.

**Table 1:** Size distribution and zeta charging of synthesized NG/SeNPs, chitosan NPs (Cht) and composite.

Nanoparticles	Size range (nm)	Mean Diameter (nm) *	$\zeta$ Potential
NG/SeNPs	3.61-35.08	13.82 <sup>a</sup>	-31.8 mV
Cht	69.56-296.62	162.16 <sup>b</sup>	+ 34.9 mV
Cht/NG/SeNPs	88.43-319.67	171.55 <sup>c</sup>	+23.6 mV

\* Means of trials' triplicates; unalike letters (superscript) within a column designate significant difference ( $p \leq 0.05$ )

$\zeta$  Potential stands for the charge of NPs which has an important effect on stability of selenium nanoparticles (Alexis *et al.*, 2008; Natrajan *et al.*, 2015). Table 1 shows the  $\zeta$  potential of SeNPs, Cht NPs, and Cht /NG/SeNPs nanocomposite which were -31.8, +34.9, and +23.6 mV, respectively. Due to the positive charge of amine groups at low pH, the Cht can be considered as a cationic and water-soluble polyelectrolyte (Losso *et al.*, 2005). Due to the presence of reducing agents such as phenolics acids and flavonoids, the SeNPs acquired the negative charged potential due to the presence of high carboxylic ions in their biosynthesized form by NG (Haznedaroglu and Zeybek, 2007; Barletta *et al.*, 2015; Abd-Elraoof *et al.*, 2023). It is important that the negatively charged NPs play an important role in the application as antimicrobial agents (Liu *et al.*, 2018). Moreover, according to Kadu *et al.*, emulsions with absolute values of differences in  $\zeta$  potential >10 mV are recommended to be more stable (Kokila *et al.*, 2017). The desirable  $\zeta$  potential values should lie within -30 to 20 mV or +20 to +30 mV (Nagalingam *et al.*, 2022).

### 3.1.4. Electron microscopy analysis

In case of the electron microscopic techniques, the visualization was done to examine the shape, Ps, and distribution of NG and SeNPs (Fig. 4A) and NC prepared with Cht (Fig. 4B). The TEM imaging indicated that NG and SeNPs prepared were mainly spherical in nature with uniform Ps and distribution (Fig. 4A). The mean diameter of the NG and SeNPs Ps obtained through imaging technique was found to be 13.91 nm. The value was similar to the result achieved through DLS analysis. Recently, harmonized results have been published (Filipović *et al.*, 2021), reporting the synthesis of spherical biogenic SeNPs with a mean Ps of 9.41 nm without much aggregation. In addition, the conjugation of Cht with NG/SeNPs can form NCs having semi-spherical shape with a mean diameter of 174.93 nm (Fig. 4B), slightly higher than that through DLS analysis.

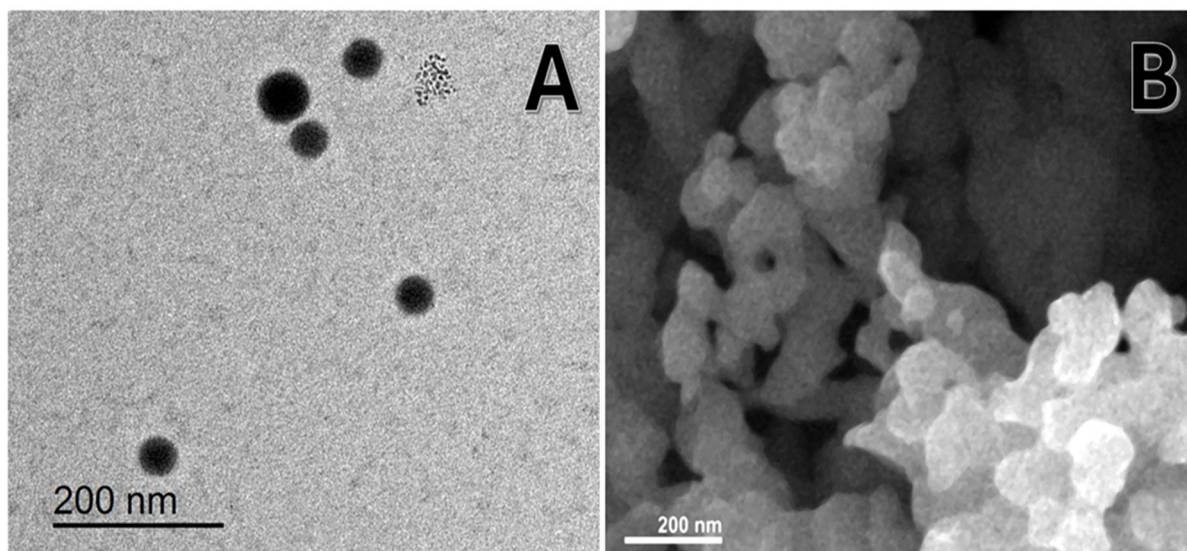


**Fig. 4:** Electron microscopy imaging of nanomaterials including TEM picture of SeNPs biosynthesized by *Posidonia oceanica* (A) and SEM of their conjugates with nanochitosan (B)

The properties of the biomolecules used for synthesizing the SeNPs, which vary according to their ability to reduce or cap SeNPs, determine the Ps, morphology, and aggregation of SeNPs formed biologically (Yuvaraj *et al.*, 2021). Ps values ranging between 2.8 and 38.9 nm were reported for SeNPs synthesized by *Spirulina platensis* microalgae (ElSaied *et al.*, 2021), while Ps values averaging at 50 nm were reported for SeNPs biosynthesized by *Catathelasma ventricosum* (Berfad *et al.*, 2021), and Ps values ranging between 3 to 18 nm were reported for SeNPs biosynthesized by raisin (*Vitis vinifera*) extract (Castellano *et al.*, 2021).

### 3.2. Antifungal activity of produced compounds

Antifungal activities against the isolates of *P. digitatum* of in vitro tested agents (Cht, NG, NG/SeNPs, and Cht/NG/SeNPs) in comparison with the standard fungicide (imazilil) were shown using both qualitative and quantitative assays for antifungal testing (Table 2). All experimented agents and compositions showed a high degree of antifungal activity against the isolated strains of *P. digitatum*. Among the tested agents/compositions, the Cht/NG/SeNPs was the highest one, and the fungicidal activities were highly significant when compared to others as well as the actions of the commercial fungicide imazilil. The synergistic antifungal action among the experimented agents was observed by the increased effectiveness of their combinations (i.e. NG/SeNPs and Cht/NG/SeNPs) compared to their individual counterparts (Cht and NG). Concerning the sensitivity of the *P. digitatum* isolates to the agents used, the isolate Pd O showed high resistance while the strain Pd 10030 was the most sensitive.

The overall antimicrobial properties, as well as specific antifungal properties, of the screened compounds were reported against different types of pathogens (Losso *et al.*, 2005; Fortunati *et al.*, 2015; Varma and Vasudevan, 2020; Salem *et al.*, 2023). Chitosan's antimicrobial property primarily relies on its positive charge, through which its interaction with the microbial membrane and its components takes place, in addition to increased ROS "reactive oxygen species" production and cellular bioactivities inhibition and cellular membranes' permeability elevation (Losso *et al.*, 2005; Salem *et al.*, 2023). Chitosan's antimicrobial activities become significantly intensified and potentiated in case of converting it to nano-biomolecule such as (Cht), due to the increased reactive surface area and small PPs size, which make their interactions more effective (Losso *et al.*, 2005; Fortunati *et al.*, 2015; Varma and Vasudevan, 2020). The antimicrobial properties of NG rely on its bioactive natural constituents such as phenolics, tannins, alkaloids, flavonoids and acids (Haznedaroglu and Zeybek, 2007; Barletta *et al.*, 2015; Vacchi *et al.*, 2017).

**Table 2:** *In vitro* antifungal evaluation of tested agents\* against isolates of *Penicillium digitatum* using minimal fungicidal concentrations (MFC, mg/mL) and inhibition zone diameter (ZOI, mm).

Antifungal compound	<i>Penicillium digitatum</i> isolates					
	<i>Pd O</i>		<i>Pd T</i>		<i>Pd 10030</i>	
	ZOI**	MFC	ZOI	MFC	ZOI	MFC
<b>Cht</b>	17.3 ± 1.4 <sup>a</sup>	35.0	18.8 ± 1.7 <sup>a</sup>	32.5	20.2 ± 1.6 <sup>a</sup>	30.0
<b>NG</b>	19.7 ± 1.6 <sup>b</sup>	32.5	22.1 ± 2.2 <sup>b</sup>	27.5	22.6 ± 2.1 <sup>b</sup>	25.0
<b>NG/SeNPs</b>	25.8 ± 2.4 <sup>c</sup>	22.5	26.3 ± 2.3 <sup>c</sup>	22.5	25.8 ± 1.8	22.5
<b>Cht/NG/SeNPs</b>	31.2 ± 2.5 <sup>d</sup>	17.5	31.8 ± 2.6 <sup>d</sup>	17.5	32.3 ± 2.9 <sup>d</sup>	15.0
<b>Imazilil</b>	24.6 ± 1.8 <sup>c</sup>	25.0	24.8 ± 2.1 <sup>c</sup>	25.0	25.4 ± 2.1 <sup>c</sup>	22.5

\* The experimented agents included nanochitosan (Cht), extract of Neptune grass (NG), biosynthesized selenium nanoparticles with NG (NG/SeNPs), and their composites, compared to standard fungicide imazilil

\*\* Dissimilar superscript letters in a column appointed significant difference at P>0.05.

The synergy among the compositing elements was found to be high and observable in Cht/NG/SeNPs, which was artistically composed in this particular study; this indicates that the composite constituents could retain their specific antifungal activity. Previous studies have also demonstrated similar findings with regard to antioxidant conjugates based on Cht and NG composites [34,68]. Moreover, the use of Cht as a carrier for other bioactive ingredients such as plant extracts, essential oils, and nanometals has been demonstrated to improve their joint performance as antibacterial or even anticancer nanocomposites (Losso *et al.*, 2005; Kokila *et al.*, 2017; Liu *et al.*, 2018; Nagalingam *et al.*, 2022).

### 3.3. Treatment of orange fruits with Cht-based edible coating

After exposure of orange fruits to infection for 10 days using *P. digitatum* O, the results obtained from treatment of the fruits using the two Cht-based edible coatings (plain Cht and Cht/NG/SeNPs) are shown in the figure below (Fig. 5). The coated fruits had lesser symptoms of infections compared to the untreated control fruits, which were totally rotten with growth of fungi (Fig. 5). Complete protection of orange fruits from any sign of infection can be achieved by coating them using Cht/NG/SeNPs solution, as well as maintaining their fresh appearance. Orange fruits treated using Cht exhibited about 24.8 ± 6.2% symptoms of infection on the fruit skin surface, whereas fruits treated using NG/SeNPs exhibited only about 4.8 ± 1.2% symptoms of fungi infestation.

Chitosan-and NCT-loaded ECs were constantly confirmed as effective tools for preventing post-harvest decay or loss of many types of agricultural products as one of their major distinguishing roles besides the antimicrobial activities, which included their ability to create barriers against new infections by fungi, retain moisture content, control fruit ripening and respiration in coated products (Yuvaraj *et al.*, 2012; Natrajan *et al.*, 2015; Berfad *et al.*, 2015; Ma *et al.*, 2017; Soltanzadeh *et al.*, 2021; Jiang *et al.*, 2021). Similarly, the NG extract played a critical role in making ECs as the major ingredient in coating many types of fruits. It possessed the ability to inhibit microbial growth on the coated fruits, keeping them fresh due to its powerful antimicrobial and antioxidant effects (Castellano *et al.*, 2012; Berfad *et al.*, 2015; Boubakri *et al.*, 2017; Abd-Elraoof *et al.*, 2023). In addition, it has been reported that the combination of chitosan and NG in making ECs might exhibit more effectiveness than using each individually (Fortunati *et al.*, 2015; Abd-Elraoof *et al.*, 2023).

The functions are proposed to have enhanced levels when Cht is conjugated with NG and used as EC in the fruits due to high capabilities of Cht to encase entire surface area of fruits, filling the pores, delivering the accompanying molecules to fruits, and protecting fruits from any fungal invasion and

quality deterioration (Soltanzadeh *et al.*, 2021; Ma *et al.*, 2017; *et al.*, 2021). In this study, Cht has been conjugated with NG/SeNPs as novel combination for use as an effective EC in orange fruit to utilize the biosafeness of Cht as well as the enhanced capability to cap as a means of providing additional properties in terms of potential biosafeness against the toxicity of SeNPs as proved in several studies (Tayel *et al.*, 2016; Jiang *et al.*, 2021; Salem *et al.*, 2022; Shehab *et al.*, 2022).

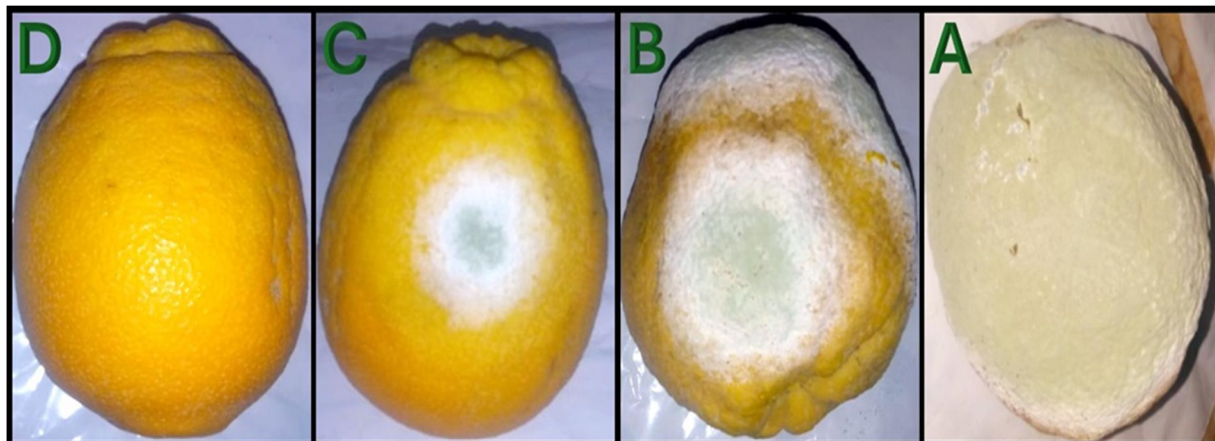


**Fig. 5:** Consequences of orange fruits coating with formulated nanochitosan (Cht; B), Cht with extract of Neptune grass (Cht/NG; C) and Cht/NG/SeNPs (D), after 10 days of infection with *Penicillium digitatum*, compared to control fruits (A)

## Conclusion

The successful manufacture of Cht, NG, and SeNPs using *P. oceanica* extract using an easy, affordable, and environmentally friendly nanobiotechnological technique was proven in this study, along with their application as antifungal and fruit preserving agents. We can draw the conclusion that Cht/NG/SeNPs nanocomposites had strong antifungal properties against citrus green mold; the nanocomposite was able to inhibit fungal cells, and their antifungal effect was successful in stopping the growth of green mold in citrus fruits. In the food business, using Cht, NG, or SeNPs as biopreservatives can be recommended. Further research is required to completely comprehend the mechanisms underlying the antifungal properties of such kinds of Cht/NG/SeNPs nanocomposites.

## References

- Abd-Elraoof, W. A., A. A. Tayel, W. Shaymaa, O. M. W. Abukhatwah, A. M. Diab, O. M. Abonama, ... and A. Abdella, 2023. Characterization and antimicrobial activity of a chitosan-selenium nanocomposite biosynthesized using *Posidonia oceanica*. RSC advances, 13(37), 26001-26014. <https://doi.org/10.1039/D3RA04288J>
- Alexis, F., E. Pridgen, L. K. Molnar and O. C. Farokhzad, 2008. Factors affecting the clearance and biodistribution of polymeric nanoparticles. Mol. Pharm. 5(4):505-15. <https://doi.org/10.1021/mp800051m>
- Ammar, N. M., H. A. Hassan, M. A. Mohammed, A. Serag, S. H. Abd El-Alim, H. Elmotasem, ... and A. H. Z. Abdel-Hamid, 2021. Metabolomic profiling to reveal the therapeutic potency of *Posidonia oceanica* nanoparticles in diabetic rats. RSC Adv., 11(14):8398-410. <https://doi.org/10.1039/D0RA09606G>
- Ashraf, M. A., W. Peng, Y. Zare and K. Y. Rhee, 2018. Effects of size and aggregation/agglomeration of nanoparticles on the interfacial/interphase properties and tensile strength of polymer nanocomposites. Nanoscale Res. Lett. 13:214. <https://doi.org/10.1186/s11671-018-2624-0>
- Bahrulolum, H., S. Nooraei, N. Javanshir, H. Tarrahimofrad, V. S. Mirbagheri, A. J. Easton and G. Ahmadian, 2021. Green synthesis of metal nanoparticles using microorganisms and their application in the agrifood sector. J Nanobiotechnology. 19(1):1-26.

- Bahrulolum, H., Nooraei, S., Javanshir, N., Tarrahimofrad, H., Mirbagheri, V. S., Easton, A. J., and Ahmadian, G. 2021. Green synthesis of metal nanoparticles using microorganisms and their application in the agrifood sector. *J. Nanobiotechnol.* 19:86.  
<https://doi.org/10.1186/s12951-021-00834-3>
- Barletta, E., M. Ramazzotti, F. Fratianni, D. Pessani and D. Degl'Innocenti, 2015. Hydrophilic extract from *Posidonia oceanica* inhibits activity and expression of gelatinases and prevents HT1080 human fibrosarcoma cell line invasion. *Cell Adh Migr.*, 9(6):422-31.  
<https://doi.org/10.1080/19336918.2015.1008330>
- Benhabiles, M. S., R. Salah, H. Lounici, N. Drouiche, M. F. A. Goosen and N. Mameri, 2012. Antibacterial activity of chitin, chitosan and its oligomers prepared from shrimp shell waste. *Food Hydrocoll.* 29(1):48-56. <https://doi.org/10.1016/j.foodhyd.2012.02.013>
- Berfad, M. A., M. A. S. Fahej, A. Kumar and S. Edrah, 2015; Preliminary phytochemical and antifungal studies of sea grass, *Posidonia oceanica* obtained from mediterranean sea of Libya. *Int. J. Sci. Res.* 4:30-3.
- Boubakri, S., M. A. Djebbi, Z. Bouaziz, P. Namour, A. Ben Haj Amara, I. Ghorbel-Abid and R. Kalfat, 2017. Nanoscale zero-valent iron functionalized *Posidonia oceanica* marine biomass for heavy metal removal from water. *Environ. Sci. Pollut. Res.* 24(36):27879-96.  
<https://doi.org/10.1007/s11356-017-0247-0>
- Britto, J., P. Barani, M. Vanaja, E. Pushpalaksmi, J. J. Samraj and G. Annadurai, 2021. Adsorption of Dyes by Chitosan-Selenium Nanoparticles: Recent Developments and Adsorption Mechanisms. *Nat. Environ. Pollut. Technol.*, 20(2):467-79. <https://doi.org/10.46488/NEPT.2021.v20i02.003>
- Castellano, G., J. Tena and F. Torrens, 2012. Classification of phenolic compounds by chemical structural indicators and its relation to antioxidant properties of *Posidonia Oceanica* (L.) Delile. *MATCH Commun. Math. Comput. Chem.*, 67:231-50.
- Chen, W., Y. Li, S. Yang, L. Yue, Q. Jiang and W. Xia, 2015. Synthesis and antioxidant properties of chitosan and carboxymethyl chitosan-stabilized selenium nanoparticles. *Carbohydr. Polym.* 132:574-81. <https://doi.org/10.1016/j.carbpol.2015.06.064>
- Cheng, Y., Y. Lin, H. Cao, and Z. Li, 2020. Citrus postharvest green mold: Recent advances in fungal pathogenicity and fruit resistance. *Microorganisms*, 8(3): 449.
- ElSaied, B. E., A. M. Diab, A. A. Tayel, M. A. Alghuthaymi and S. H. Moussa, 2021. Potent antibacterial action of phycosynthesized selenium nanoparticles using *Spirulina platensis* extract. *Green Process. Synth.*, 10(1):49-60. <https://doi.org/10.1515/gps-2021-0005>
- FAOSTAT (2020). FAO Statistics, Food and Agriculture Organization of the United Nations, Rome, Italy. Accessed 22 December 2021. <https://www.fao.org/faostat/en/#home>
- Filipović, N., D. Ušjak, M. T. Milenković, K. Zheng, L. Liverani, A. R. Boccaccini and M. M. Stevanović, 2021. Comparative study of the antimicrobial activity of selenium nanoparticles with different surface chemistry and structure. *Front. Bioeng. Biotechnol.* 8:624621.  
<https://doi.org/10.3389/fbioe.2020.624621>
- Fortunati, E., F. Luzi, D. Puglia, R. Petrucci, J. M. Kenny, and L. Torre, 2015. Processing of PLA nanocomposites with cellulose nanocrystals extracted from *Posidonia oceanica* waste: Innovative reuse of coastal plant. *Ind Crops Prod.*, 67:439-47. <https://doi.org/10.1016/j.indcrop.2015.01.075>
- Ganachari, S. V., J. S. Yaradoddi, S.B. Somappa, P. Mogre, R.P. Tapaskar, B. Salimath, ... and V. J. Viswanath, 2019. Green nanotechnology for biomedical, food, and agricultural applications. In: Martínez L, Kharissova O, Kharisov B, editors. *Handbook of Ecomaterials*. Springer, Cham, p 2681–98.
- Haghighi, M., Yazdanpanah, S. 2020. Chitosan-based coatings incorporated with cinnamon and tea extracts to extend the fish fillets shelf life: Validation by FTIR spectroscopy technique. *J. Food Qual.* 2020: 8865234. <https://doi.org/10.1155/2020/8865234>.
- Hariharan, H., N. Al-Harbi, P. Karuppiyah and S. Rajaram, 2012. Microbial synthesis of selenium nanocomposite using *Saccharomyces cerevisiae* and its antimicrobial activity against pathogens causing nosocomial infection. *Chalcogenide Lett.*, 9(12):509-15.
- Haznedaroglu, M.Z., and U. Zeybek, 2007. HPLC Determination of Chicoric Acid in Leaves of *Posidonia oceanica*. *Pharm. Biol.* 45(10):745-8. <https://doi.org/10.1080/13880200701585717>
- He, X., H. Deng and H.M. Hwang, 2019. The current application of nanotechnology in food and agriculture. *J Food Drug Anal.*, 27(1):1-21.

- Huang, H., Q. Yuan and X. Yang, 2004. Preparation and characterization of metal–chitosan nanocomposites. *Colloids Surf. B* . 39(1-2):31-7. <https://doi.org/10.1016/j.colsurfb.2004.08.014>
- Jha, R., and R.A. Mayanovic, 2023. A Review of the Preparation, Characterization, and Applications of Chitosan Nanoparticles in Nanomedicine. *Nanomaterials* 13, 1302. <https://doi.org/10.3390/nano13081302>
- Jiang, M., Y. Song, M. K. Kanwar, G. J. Ahammed, S. Shao and J. Zhou, 2021. Phytonanotechnology applications in modern agriculture. *J. Nanobiotechnol.* 19(1): 430. <https://doi.org/10.1186/s12951-021-01176-w>.
- Kumar, A., A. Choudhary, H. Kaur, S. Mehta and A. Husen, 2021. Metal-based nanoparticles, sensors, and their multifaceted application in food packaging. *J Nanobiotechnology.* 19(1):1-25.
- Kannan, S., K. Mohanraj, K. Prabhu, S. Barathan, and G. Sivakumar, 2014. Synthesis of selenium nanorods with assistance of biomolecule. *Bull. Mater. Sci.* 37(7):1631-5. <https://doi.org/10.1007/s12034-014-0712-z>
- Khan, I., K. Saeed and I. Khan, 2019. Nanoparticles: Properties, applications and toxicities. *Arab. J. Chem.*, 12(7):908-31. <https://doi.org/10.1016/j.arabjc.2017.05.011>
- Kharchoufi, S., L. Parafati, F. Licciardello, G. Muratore, M. Hamdi, G. Cirvilleri, , and Restuccia, C. 2018. Edible coatings incorporating pomegranate peel extract and biocontrol yeast to reduce *Penicillium digitatum* postharvest decay of oranges. *Food Microbiol.*, 74:107-12.
- Khoerunnisa, F., Y. D. Yolanda, M. Nurhayati, F. Zahra, M. Nasir, P. Opaprakasit, , ... and E. P. Ng, 2021. Ultrasonic Synthesis of Nanochitosan and Its Size Effects on Turbidity Removal and Dealkalization in Wastewater Treatment. *Invent.* 6(4):98. <https://doi.org/10.3390/inventions6040098>
- Khot, L. R., S. Sankaran, J. M. Maja, R. Ehsani and E. W. Schuster, 2012. Applications of nanomaterials in agricultural production and crop protection: a review. *Crop Prot.*, 35:64-70.
- Khurana, A., S. Tekula, M. A. Saifi, P. Venkatesh and C. Godugu, 2019. Therapeutic applications of selenium nanoparticles. *Biomed. Pharmacother.*, 111:802-12. <https://doi.org/10.1016/j.biopha.2018.12.146>
- Kokila, K., N. Elavarasan and V. Sujatha, 2017. *Diospyros montana* leaf extract-mediated synthesis of selenium nanoparticles and their biological applications. *New J Chem.* 41(15):7481-90. <https://doi.org/10.1039/C7NJ01124E>
- Liu, H. J., C. H. Xu, W. M. Li, F. Wang, Q. Zhou, A. Li, ... and S. Q. Sun, 2013. Analysis of *Spirulina* powder by Fourier transform infrared spectroscopy and calculation of protein content. *Spectrosc. Spectr. Anal.*, 33(4):977-81. [https://doi.org/10.3964/j.issn.1000-0593\(2013\)04-0977-05](https://doi.org/10.3964/j.issn.1000-0593(2013)04-0977-05)
- Liu, Y., S. Zeng, Y. Liu, W. Wu, Y. Shen, L. Zhang, ... and C. Wang, 2018. Synthesis and antidiabetic activity of selenium nanoparticles in the presence of polysaccharides from *Catathelasma ventricosum*. *Int. J. Biol. Macromol.* 114:632-9. <https://doi.org/10.1016/j.ijbiomac.2018.03.161>
- Losso, J. N., A. Khachatryan, M. Ogawa, J. S. Godber and F. Shih, 2005. Random centroid optimization of phosphatidylglycerol stabilized lutein-enriched oil-in-water emulsions at acidic pH. *Food Chem.* 92(4):737-44. <https://doi.org/10.1016/j.foodchem.2004.12.029>
- Ma, Z., A. Garrido-Maestu and K. C. Jeong, 2017. Application, mode of action, and in vivo activity of chitosan and its micro-and nanoparticles as antimicrobial agents: A review. *Carbohydr. Polym.*, 176:257-65. <https://doi.org/10.1016/j.carbpol.2017.08.082>
- Marrie, T.J., J.W. Costerton, 1984. Scanning and transmission electron microscopy of in situ bacterial colonization of intravenous and intraarterial catheters. *J. Clin. Microbiol.*, 19(5):687-93.
- Mellinas, C., A. Jiménez and M. D. C. Garrigós, 2019. Microwave-assisted green synthesis and antioxidant activity of selenium nanoparticles using *Theobroma cacao* L. bean shell extract. *Molecules.* 24(22):4048. <https://doi.org/10.3390/molecules24224048>
- Meneses, C. C. F., P. R. M. de Sousa, K. C. N. Lima, L. M. M. D. A.Souza, W. P. Feio, C. M. R. Remédios, , ... and M. C. Monteiro, 2023. Caffeic Acid-Zinc Basic Salt/Chitosan Nanohybrid Possesses Controlled Release Properties and Exhibits In Vivo Anti-Inflammatory Activities. *Molecules*, 28, 4973. <https://doi.org/10.3390/molecules28134973>
- Nagalingam, M., S. Rajeshkumar, S. K. Balu, M. Tharani, and K. Arunachalam, 2022.; Anticancer and Antioxidant Activity of *Morinda citrifolia* Leaf Mediated Selenium Nanoparticles. *J. Nanomater.*, 2022. <https://doi.org/10.1155/2022/2155772>

- Natrajan, D., S. Srinivasan, K. Sundar and A. Ravindran, 2015. Formulation of essential oil-loaded chitosan–alginate nanocapsules. *JFDA*. 23(3):560-8. <https://doi.org/10.1016/j.jfda.2015.01.001>
- Nayak, V., K. R. Singh, A. K. Singh and R. P. Singh, 2021. Potentialities of selenium nanoparticles in biomedical science. *New J Chem.*, 45(6):2849-78. <https://doi.org/10.1039/D0NJ05884J>
- Pelgrift, R.Y. and A.J. Friedman, 2013. Nanotechnology as a therapeutic tool to combat microbial resistance. *Adv. Drug Deliv. Rev.* 65(13-14):1803-15. <https://doi.org/10.1016/j.addr.2013.07.011>
- Pulido, R., L. Bravo and F. Saura-Calixto, 2000. Antioxidant activity of dietary polyphenols as determined by a modified ferric reducing/antioxidant power assay. *J. Agric. Food Chem.*, 48(8):3396-402. <https://doi.org/10.1021/jf9913458>
- Rao, S., Y. Lin, R. Lin, J. Liu, H. Wang, W. Hu, , ... and T. Chen, 2022. Traditional Chinese medicine active ingredients-based selenium nanoparticles regulate antioxidant selenoproteins for spinal cord injury treatment. *J. Nanobiotechnol.* 20: 278. <https://doi.org/10.1186/s12951-022-01490-x>
- Salem, M.F., W.A. Abd-Elraoof, A.A. Tayel, F.M. Alzuair and O.M. Abonama, 2022. Antifungal application of biosynthesized selenium nanoparticles with pomegranate peels and nanochitosan as edible coatings for citrus green mold protection. *J. Nanobiotechnol.*, 20:182. <https://doi.org/10.1186/s12951-022-01393-x>
- Saratale, R. G., I. Karuppusamy, G. D. Saratale, A. Pugazhendhi, G. Kumar, Y. Park, ... and H. S. Shin, 2018. A comprehensive review on green nanomaterials using biological systems: Recent perception and their future applications. *Colloids Surf B.*, 170:20-35.
- Sharma, V.P., U. Sharma, M. Chattopadhyay and V.N. Shukla, 2018. Advance applications of nanomaterials: a review. *Mater Today: Proc.*, 5(2):6376-80.
- Shehab, M.M., Z.I. Elbially, A.A. Tayel, S.H. Moussa, and I.I. Al-Hawary, 2022. Quality Boost and Shelf-Life Prolongation of African Catfish Fillet Using *Lepidium sativum* Mucilage Extract and Selenium Nanoparticles. *J. Food Qual.*, 2022: 9063801. <https://doi.org/10.1155/2022/9063801>.
- Soltanzadeh, M., S. H. Peighambaroust, B. Ghanbarzadeh, M. Mohammadi and J. M. Lorenzo, 2021. Chitosan nanoparticles as a promising nanomaterial for encapsulation of pomegranate (*Punica granatum* L.) peel extract as a natural source of antioxidants. *J. Nanomater.* 11(6):1439. <https://doi.org/10.3390/nano11061439>
- Tayel, A. A., A. F. Elzahy, S. H. Moussa, M. S. Al-Saggaf, and A. M. Diab, 2020. Biopreservation of shrimps using composed edible coatings from chitosan nanoparticles and cloves extract. *J. Food Qual.*, 2020. <https://doi.org/10.1155/2020/8878452>
- Tayel, A. A., Moussa, S. H., Salem, M. F., Mazrou, K. E., and El-Tras, W. F. 2016. Control of citrus molds using bioactive coatings incorporated with fungal chitosan/plant extracts composite. *J. Sci. Food Agric.* 96(4):1306-12.
- Tayel, A. A., Moussa, S., Opwis, K., Knittel, D., Schollmeyer, E., and Nickisch-Hartfiel, A. 2010. Inhibition of microbial pathogens by fungal chitosan. *Int. J. Biol. Macromol.* 47(1):10-4. <https://doi.org/10.1016/j.ijbiomac.2010.04.005>
- Tayel, A.A., El-Baz A.F., Salem M.F., El-Hadary, M.H. 2009. Potential applications of pomegranate peel extract for the control of citrus green mold. *J Plant Dis Protect.*, 116:252–6.
- Torres, S. K., V. L. Campos, C. G. León, S. M. Rodríguez-Llamazares, S. M. Rojas, M. González, , ... and M. A. Mondaca, 2012. Biosynthesis of selenium nanoparticles by *Pantoea agglomerans* and their antioxidant activity. *J. Nanoparticle Res.* 11(3):463. <https://doi.org/10.3390/biology11030463>
- Tripathi, P., N.K. Dubey, 2004. Exploitation of natural products as an alternative strategy to control postharvest fungal rotting of fruit and vegetables. *Postharvest Biol Technol.*, 32(3):235-45.
- Vacchi, M., G. De Falco, S. Simeone, M. Montefalcone, C. Morri, M. Ferrari and C. N. Bianchi, 2017. Biogeomorphology of the Mediterranean *Posidonia oceanica* seagrass meadows. *Earth Surf. Process. Landf.* 42(1):42-54. <https://doi.org/10.1002/esp.3932>
- Varma, R., and S. Vasudevan, 2020. Extraction, characterization, and antimicrobial activity of chitosan from horse mussel *Modiolus modiolus*. *ACS omega.* 5(32):20224-30. <https://doi.org/10.1021/acsomega.0c01903>
- Wang, Z., Y. Sui, J. Li, X. Tian and Q. Wang, 2020. Biological control of postharvest fungal decays in citrus: a review. *Crit Rev Food Sci Nutr.*, 62(4):861-870.

- Yu, Y., P. Fan, J. Li and S. Wang, 2023. Preparation of Biocompatible Manganese Selenium-Based Nanoparticles with Antioxidant and Catalytic Functions. *Molecules*. 28, 4498.  
<https://doi.org/10.3390/molecules28114498>
- Yuvaraj, N., P. Kanmani, R. Satishkumar, A. Paari, V. Pattukumar and V. Arul, 2012. Seagrass as a potential source of natural antioxidant and anti-inflammatory agents. *Pharm. Biol.* 50(4):458-67.  
<https://doi.org/10.3109/13880209.2011.611948>
- Zhai, X., C. Zhang, G. Zhao, S. Stoll, F. Ren, and X. Leng, 2017. Antioxidant capacities of the selenium nanoparticles stabilized by chitosan. *J. Nanobiotechnol.* 15:4.  
<https://doi.org/10.1186/s12951-016-0243-4>
- Zhang, N., Q. Ping, G. Huang, W. Xu, Y. Cheng and X. Han, 2006. Lectin-modified solid lipid nanoparticles as carriers for oral administration of insulin. *Int. J. Pharm.* 327(1-2):153-9.  
<https://doi.org/10.1016/j.ijpharm.2006.07.026>.